

Terahertz microjets and graphene: Technologies towards ultrafast all-optical modulation

Mark H. Bergen, Brandon Born, Simon Geoffroy-Gagnon, and Jonathan F. Holzman

The University of British Columbia, School of Engineering, 3333 University Way, Kelowna, BC, Canada, V1V 1V7

Abstract—Key technologies for ultrafast all-optical THz modulation are introduced. A graphene monolayer is applied for modulation, on a picosecond timescale, and a dielectric sphere is applied to form a high-intensity THz microjet within the graphene monolayer.

Radio-frequency technology (RF) is the backbone of modern wireless communications. It has supported the rapid growth in demand for wireless communications over the past decade, which has manifested itself as a doubling of data rates every 18 months [1]. There is a challenge for continuing such growth, however, in that the licensed RF spectrum has a limited range of 3 kHz to 300 GHz. Alternative modulation schemes, such as high-order quadrature amplitude modulation [2], have been applied to squeeze data into the contiguous licensed bands below 300 GHz, but capacity limitations and spectrum scarcity are growing concerns [3].

A solution to the above challenges may lie in the terahertz (THz) band operating above RF frequencies. This THz band, spanning frequencies from 300 GHz to 10 THz, has notable benefits. It has sufficiently high frequencies to allow for unlicensed operation and high data rates. At the same time, it has sufficiently low frequencies to enable coherent generation and detection of electric fields—by way of antennas that are tailored to the amplitude and phase characteristics of the THz band. However, key technologies are still needed to realize effective THz wireless communication systems.

One of the key technologies needed to realize effective THz wireless communications is modulation. The applied modulation scheme must accommodate the unique refraction and absorption characteristics of radiation in the THz band. At the same time, it must be sufficiently fast to function with the high data rates and broad bandwidths of the THz band. Various electronic THz modulation schemes have been demonstrated in the past. The technologies have been based on high electron mobility transistor structures [4], phase modulators [5], split ring resonators [6], and others.

A particularly effective approach to THz modulation has come about in recent years in the form of all-optical modulation. All-optical THz modulation benefits from its ability to transfer optically-encoded data, typically from the 1550 nm communications band of fibre optic cables, directly to wirelessly broadcasted THz signals. Various forms of all-optical THz modulation have emerged in recent years, based on photonic crystals [7], and semiconductors [8].

In this work, a new all-optical THz modulation scheme is proposed and analysed. The proposed scheme uses a graphene monolayer as the optically-active material. The graphene monolayer allows a near-infrared (near-IR) control beam to modulate a co-incident THz beam. The proposed scheme also uses a dielectric sphere, with an appropriate refractive index and diameter, to form a high-intensity THz microjet within the graphene monolayer at its rear surface. The intense focusing yields a sub-wavelength THz beamspot size, which in turn

allows the co-incident near-IR control beam to be applied with an equally small beamspot size. This lowers the demand on switching fluence of the near-IR control beam and enhances the depth of modulation on the THz beam. Developmental results are presented. Characterizations are shown of the graphene monolayer, following photoexcitation by the near-IR control beam, and the THz microjet, for spheres with varying diameters and refractive indices.

The proposed all-optical THz modulation scheme is shown in Fig. 1. The figure shows a dielectric sphere with a diameter of $d = 0.75$ mm and refractive index of $n = 1.53$. Mie theory is applied to study the focal characteristics of the sphere [9]. The Mie theory results are shown as greyscale intensities in the figure, given illumination on the left (front) surface of the sphere by a collimated THz beam with a frequency of $f = 1$ THz and corresponding free-space wavelength of $\lambda_0 = 293$ μm . The THz beam is focused by the dielectric sphere to form a THz microjet, with a 176- μm -diameter beamspot, within the graphene monolayer on the right (rear) surface of the sphere. The THz microjet is the long-wavelength analog to the photonic nanojet that is formed via focusing by micron-scale dielectric spheres at visible and near-infrared wavelengths [9]. For the present case, with scaling up to the long wavelengths of THz beams, it becomes necessary to use dielectric spheres with millimetre-scale diameters.

The material response of the graphene monolayer is analysed first. Graphene is selected because of its unique bandstructure. Unlike typical semiconductors, which exhibit a parabolic bandstructure and a nonzero bandgap, graphene exhibits a bandstructure having two (Dirac) cones that touch at the apex (Dirac) point. This establishes a linear energy-momentum dispersion relationship with a bandgap of zero. Thus, for all-optical modulation, a pump (control) beam and

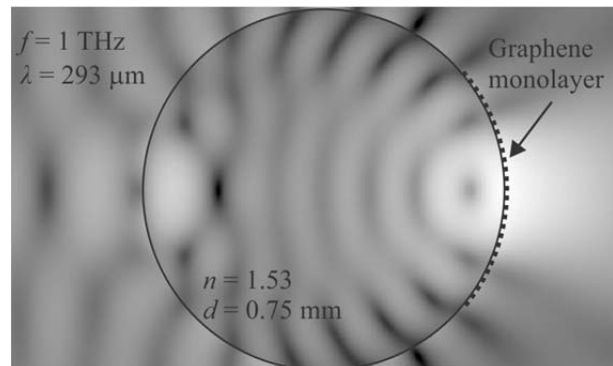


Fig. 1 The all-optical THz modulation scheme. Numerical results from Mie theory are shown as greyscale intensities for a dielectric sphere with a diameter of $d = 0.75$ mm and refractive index of $n = 1.53$. The left (front) surface of the sphere is illuminated by a THz beam with a frequency of $f = 1$ THz and a corresponding free-space wavelength of $\lambda_0 = 293$ μm . The THz beam is focused as a THz microjet within the graphene monolayer on the right (rear) surface of the sphere.

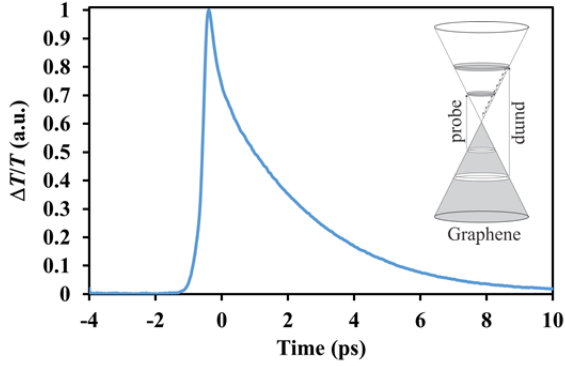


Fig. 2 Experimental results for ultrafast all-optical modulation of a graphene monolayer. Differential transmission of a 1550 nm probe beam, $\Delta T/T$, is shown as a function of time for photoexcitation by a 780 nm pump beam. The inset shows the graphene bandstructure under pump and probe excitation.

probe (signal) beam can be used to photoexcite electrons from the valence band to the conduction band at high and low states, respectively. The pump-excited electrons undergo energy relaxation down through the states receiving the probe-excited electrons. This process manifests itself as a pump-induced decrease in the probe beam absorption due to Pauli blocking, i.e., state filling, which is seen as a pump-induced increase in the probe beam transmission. The process is shown in the inset of Fig. 2. The timescale for recovery of the change in the probe beam transmission is defined by the time constant for energy relaxation of the pump-excited electrons.

To define the prospects of ultrafast all-optical modulation with graphene, a time-resolved pump-probe experiment is implemented. The experiment uses a 780 nm pump beam and a 1550 nm probe beam, each of which has 100 fs pulses with a repetition rate of 90 MHz. The results are shown in Fig. 2. The figure shows the differential probe transmission, $\Delta T/T$, as a function of time. The results show that the energy relaxation time of the electrons is on a picosecond timescale, with a time constant of 2.3 ps, which agrees with prior studies [10]. This defines a lower limit of the switching time for the application of this material to ultrafast all-optical modulation.

The refractive response of the dielectric sphere is analysed next. The THz microjet intensity, being defined by as the intensity of THz beam on the optical axis at the rear surface of the dielectric sphere (within the graphene monolayer) is computed via Mie theory simulations. The simulations are carried out for a wide range of values for the diameter, d , and refractive index, n , of the dielectric sphere. Representative results are shown in Fig. 3. The figure shows the normalized THz microjet intensity as a function of the frequency, f . The results are shown for a dielectric sphere with diameter of $d = 5$ mm and refractive indices of $n = 1.6, 1.7, 1.8, 1.9$, and 2.0 . It becomes clear from the presented results that a refractive index of $n = 1.8$ creates an optimal THz microjet, i.e., a THz microjet with high intensities across a broad frequency range. This observation is part of a larger trend—which is not shown but is described here. When the diameter of the dielectric sphere is much larger than the wavelength, the optimal THz microjet is formed for a refractive index of $n \approx 2$. This comes

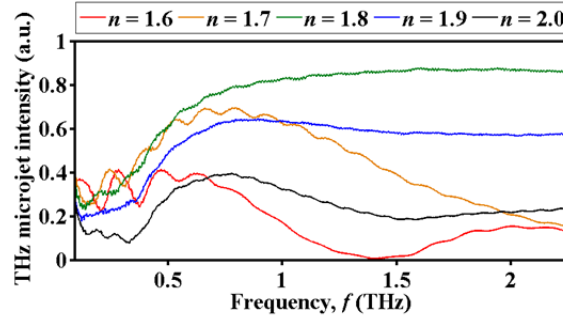


Fig. 3 Normalized THz microjet intensity in the graphene monolayer, i.e., on the optical axis at the rear surface of the dielectric sphere, versus frequency. The results are shown for a dielectric sphere with a diameter of $d = 5$ mm and refractive indices of $n = 1.6, 1.7, 1.8, 1.9$, and 2.0 .

about from the limiting case of ray theory [9]. As the diameter of the dielectric sphere is reduced, however, the refractive index that forms the optimal THz microjet is also reduced. For the present case, with a sphere having a diameter of $d = 5$ mm, the ideal THz microjet requires a refractive index of $n = 1.8$. However, in general, it will be necessary to select the diameter and material of the dielectric sphere according to both the refractive index (to form the optimal THz microjet) and extinction coefficient (to minimize losses in the THz band).

In conclusion, an effective all-optical THz modulation scheme was put forward in this work. A graphene monolayer was introduced as a material for modulation. A dielectric sphere was introduced as a structure for creating a high-intensity THz microjet within the graphene monolayer at the rear of the sphere—but only given appropriate consideration to the refractive index and diameter of the sphere. Our future studies in this work will include the demonstration and characterization of the fully-integrated all-optical THz modulator.

- [1] S. Cherry, "Edholm's Law of bandwidth," *IEEE Spectr.*, vol. 41, pp. 58-60, 2004.
- [2] Seeds *et al.*, "Terahertz photonics for wireless communications," *J. Lightw. Technol.*, vol. 33, pp. 579-587, 2015.
- [3] Akyildiz *et al.*, "Terahertz band: Next frontier for wireless communications," *Phys. Commun.*, vol. 12, pp. 16-32, 2014.
- [4] Kleine-Ostmann *et al.*, "Room-temperature operation of an electrically driven terahertz modulator," *Appl. Phys. Lett.*, vol. 84, no. 18, pp. 3555-3557, 2004.
- [5] Chen *et al.*, "A metamaterial solid-state terahertz phase modulator," *Nature Photon.*, vol. 3, no. 3, pp. 148-151, 2009.
- [6] D. Mittleman, "A terahertz modulator," *Nature*, vol. 444, no. 7119, pp. 560-561, 2006.
- [7] Fekete *et al.*, "Ultrafast opto-terahertz photonic crystal modulator," *Opt. Lett.*, vol. 32, no. 6, pp. 680-682, 2007.
- [8] Nozokido *et al.*, "Modulation of submillimeter wave radiation by laser-produced free carriers in semiconductors," *Electron. Comm. Jpn.*, vol. 80, pp. 1-9, 1997.
- [9] Born *et al.*, "Integration of photonic nanojets and semiconductor nanoparticles for enhanced all-optical switching," *Nature Commun.*, vol. 6, pp. 8097(1-9), 2015.
- [10] Breusing *et al.*, "Ultrafast carrier dynamics in graphite," *Phys. Rev. Lett.*, vol. 102, no. 8, pp. 086809, 2009.